WESTERN REGION TECHNICAL ATTACHMENT
NO. 98-24
JULY 7, 1998

USE OF THERMODYNAMIC INFORMATION TO PREDICT LOW-REFLECTIVITY MICROBURSTS

Steve Vasiloff
NOAA/ERL/NSSL - NWS/WR/SSD

Stacy Stewart
NWS/OSF/OTB

Mike Splitt
University of Utah

Introduction

Predicting maximum winds during dry microburst events is made difficult by their small temporal and spatial scales. As discussed by Vasiloff (1997) and Vasiloff and Hogan (1997), classical radar microburst precursors are a descending reflectivity core and convergence near or above cloud base. While convergence at or just above cloud base generally accompanies downdrafts that produce microbursts, it often develops after the core has started to descend and results in short lead times for warning. Still, the development of strong convergence indicates a change in the dynamic structure of the microburst cell and may indicate that stronger subsequent events will occur.

To improve warning lead times, this Technical Attachment (TA) explores a gust prediction technique (GPT) derived from a 1-D cloud model in a paper published by Srivastava (1985). Two cells in northern Utah are used to test the technique. The conclusions in this TA are based on a simple model of a dry-microburst storm where a single reflectivity core produces a downdraft as it descends.

An important part of the warning process is quick recognition and diagnosis of important cells by the WSR-88D algorithms. It is shown that a reflectivity threshold reduction in the storm cell identification and tracking (SCIT) algorithm is necessary to allow the forecaster access to important information about the cells' structure and history. However, without the inclusion of the GPT, the lower thresholds will produce too many cells for the forecaster to keep track of.

Gust Prediction Technique

A microburst is the result of negative buoyancy produced when precipitation evaporates/sublimates into dry air below cloud base (e.g., Roberts and Wilson 1989). A typical "inverted-V" sounding can be seen in Brown et al., (1982) and Vasiloff (1997). Srivastava (1985) used a 1-dimensional cloud model to determine important sounding parameters which included (a) a mean sub-cloud lapse rate (SCLR) and (b) the 550 mb temperature, and (c) a penetrative depth of 3.7 km. A Marshall-Palmer drop size distribution and liquid -only processes were assumed. From the model results, Srivastava noted that "the intensity of the downdraft, at the bottom of the column [near the surface], increase(d) with 1) increasing lapse rate of temperature in the environment, 2) increasing rainwater mixing ratio at the top of the downdraft, 3) increasing relative humidity of the environment and 4) decreasing raindrop size; it decreases with increasing mixing of environmental air into the downdraft." The use of Srivastava's GPT results in a maximum downdraft velocity (ms^{-1}) in terms of (a) peak radar reflectivity in dBZ, (b) a sub-cloud lapse rate, and (c) vertical distance to the ground. The final assumption is that, upon reaching the ground, the downdraft will spread out horizontally with a peak gust equal to that of the peak velocity of the steady-state downdraft. While this technique is used to predict peak wind gusts associated with dry/low-reflectivity microbursts, the same thermodynamic reasoning has also been applied to wet microbursts (Stewart, 1991 a, b; 1996).

An important caveat is that Srivastava's model did not include ice. Ice processes will produce a colder downdraft and stronger surface winds. Unfortunately, the WSR-88D does not discriminate between water and ice. Further data will be needed to determine the effect of the water-only assumption.

Case Studies

Data from dry microburst cases of 9 July 1997 (Vasiloff and Hogan, 1997) and 27 July 1996 are used to demonstrate the GPT. Srivastava's Fig. 5a regarding the core's peak reflectivity value versus maximum downdraft speed (i.e., peak gust) is shown in Fig 1. and reproduced in Table 1. Lapse rates <-9.6 Ckm^{-1} have been extrapolated. An important point to note is that more-stable lapse rates require higher cloud water content to produce the same downdraft speed (or wind gust).DDPDA look-up table

9 July 1997 Case

In the 9 July case, strong surface winds were preceded by a descending core and weak radial convergence (Fig. 2). This storm was ~55 nm from the KMTX WSR-88D near the Great Salt Lake. The reflectivity core descent began before the convergence signature developed in the Doppler velocity data (~6 ms^{-1}). Thus, reflectivity data were a better predictor. In fact, even though there was weak convergence evident in the radial velocity field, the NSSL convergence detection algorithm failed to find ANY convergence with this cell.

A maximum reflectivity value of 32 dBZ was observed at a height of 18,300 ft AGL at 2232 UTC. A SCLR of -9.7 Ckm^{-1} and a cloud base of 15,000 ft above radar level (ARL) were computed from the 0000 UTC sounding (Fig. 3). Cloud base was just above the freezing level. Using Table 1, a maximum downdraft velocity or peak wind gust up to 25 ms^{-1} (50 kt) was expected. At 2310 UTC, a spotter recorded an anemometer gust of 56 mph (48.7 kt). An effective lead time of more than 30 minutes was realized. One of the authors observed the microburst and noticed that the impact was 2-3 miles from the location of the report. Thus, the actual lead-time was more likely on the order of 20 minutes.

In addition to monitoring vertical cross sections, forecasters can monitor cell trends (if the cell is detected). Time-height and time trends of reflectivity for this cell (Figs. 4 and 5, respectively) indicate the core's descent near 2233 UTC. Note the increase in reflectivity as the core descends below the melting level.

Table 1. Table of predicted surface gusts (ms^{-1}) as a function of reflectivity and sub-cloud lapse rate. Data are from Srivastava (1985) and have been re-mapped into discrete categories to facilitate use during operations.

Lapse rate	Core value (dBZ)					
C/km	25-28	28.5-32	32.5-36	36.5-41.5	42-47	47.5-52
-8.5 to -8.7	-	-	<10	<15	<18	<25
-8.8 to -9.00	-	<15	<18	<20	<25	<30
-9.1to -9.3	<15	<18	<20	<22	<26	<32
-9.4 to -9.6	<19	<21	<22	<23	<27	<33
-9.7 to -10.	<22	<25	<27	<29	<31	<38
-10.1 to -10.5	<25	<28	<29	<31	<34	<40

27 July 1996 Case

The GPT was also applied to a 27 July 1996 dry microburst about 70 nm from KMTX. This microburst occurred over the Dugway mesonet run by the U.S. Army. A maximum reflectivity value of 47 dBZ was observed at a height of 18,000 ft AGL at 2202 UTC (Fig. 6). A SCLR of -8.7 Ckm^{-1} and a cloud base of 15,000 ft were computed from the 0000 UTC sounding (Fig. 7). Using Table 1, a maximum downdraft velocity or peak wind gust up to 18 ms^{-1} (36 kt) was expected. A 20 ms^{-1} (41 kt) gust was observed at 2315 UTC. The microburst core passed ~4 nm to the west of the site. The distance between the impact zone and the mesonet site results in reduced confidence in leadtime or accuracy of the prediction. Other sites recorder lesser gusts.

This is an important case in that, if high reflectivity were the only factor considered, a false alarm would have occurred. However, a weaker gust was predicted (and occurred) because of the less-steep lapse rate.

Another factor in this case was that the Doppler convergence signature was contaminated with range-folded velocities and therefore useless. Thus, reflectivity was the only information available - even if there had been a strong convergence signature.

As with the 9 July case, time-height and time trends of reflectivity indicated the core's descent (Figs. 8 and 9, respectively). In this case, the beginning of the cell's descent occurred near 2205 UTC. Again, note the increase in reflectivity as the core descends below the melting level.

Detection of Low-reflectivity Storms by the WSR-88D SCIT Algorithm

The default minimum reflectivity value for identifying a cell in the SCIT algorithm is 30 dBZ over an area of at least 10 km^{-2}. However, during summer months storms in the West often have peak reflectivities below these thresholds. If that happens, other attributes associated with the weak cell, even if a different algorithm finds a signature (e.g., mid-level convergence and cell reflectivity trends), will not be made available to the radar operator. The S. Jordan cell of 9 July 1997, described above, was never detected as a cell using default thresholds in the SCIT algorithm. The 27 July 1996 cell was detected only after the core began to descend.

Data from both cases were re-processed with lower SCIT thresholds. There are actually several levels of reflectivity thresholds in the parameter file (for more information on how the algorithms work, see WATADS documentation). For this case, the array of thresholds was set as follows: 36-40 dBZ; 32-36 dBZ; 28-32 dBZ; 24-28 dBZ; 20 -24 dBZ; and 16-20 dBZ. Thus, the minimum value is 16 dBZ. Also, the array indicates that anything greater than 40 dBZ will all be one cell even though there may be smaller cells imbedded inside the 40 dBZ area, as in some Midwestern squall lines. For those wishing to use WATADS to perform these types of studies, it is important to note that even though the parameter window won't allow reflectivities less than 30 dBZ, the ssaparm.dat file can be modified with the results shown in the parameter window (Fig. 10).

The reduction of the minimum reflectivity threshold from 30 dBZ to 16 dBZ resulted in a 300-500% increase in the number of cells detected in both cases. In the 9 July case, the 16 dBZ threshold resulted in the detection of six previously undetected cells in a small complex (Fig. 11). The S. Jordan cell (cell ID 13) was detected beginning with the volume scan just prior to the cell's core descent. Recalling the GPT, this is critical because the forecaster MUST know when the core is at its peak height and reflectivity.

In the 27 July case, the reduced thresholds resulted in seven additional cells detected in a complex similar to the one on 9 July (Fig. 12). Cells 89, 93, and 95 were detected with the 30 dBZ minimum threshold. However, the threshold reduction allowed the microburst-producing cell (#93) to be detected before the core began to descend.

An important caveat is that with reduced SCIT thresholds, there will be many more cells in the cell table. The GPT must be added to the algorithm suite in order for the forecaster to know which cells are important. Otherwise, an overabundance of weak cells will overwhelm the forecaster.

Forecaster Guidance

To use the GPT, the forecaster needs to follow these steps:

a) Determine the SCLR from the morning sounding and surface observations; and

b) Determine the peak reflectivity in the core aloft **above** cloud base.

- Reflectivity values $\geq$ 50 dBZ will likely result in severe surface wind gusts regardless of the SCLR.

- Weaker reflectivities require steeper lapse rates.

EXAMPLES

- A core reflectivity of 40 dBZ and a SCLR <-10.5 C km^{-1} can produce a gust of 62 kt

- A core reflectivity of 40 dBZ and a SCLR <-9.5 C km^{-1} can produce a gust of 46 kt

- A core reflectivity of 40 dBZ and a SCLR <-8.5 C km^{-1} can produce a gust of 30 kt

- A core reflectivity of 28 dBZ and a SCLR <-10.5 C km^{-1} can produce a gust of 56 kt

- A core reflectivity of 28 dBZ and a SCLR <-9.5 C km^{-1} can produce a gust of 42 kt

- A core reflectivity of 28 dBZ and a SCLR <-8.5 C km^{-1} will produce negligible winds

For a given reflectivity value, small changes in lapse rate have a large effect on the predicted gust.

In both microburst cases presented earlier, the reflectivity maximum occurred several minutes before the cloud-base convergence signature developed which resulted in a greater warning lead time. Based on a core descent of 1000 ft per minute, the GPT should yield lead times of 15 minutes or more. Additional lead time is possible for locations away from the impact area, although the wind speeds may decrease as the outflow spreads out due to frictional effects.

Considering that, in both cases, the radar echo peaked in value and altitude several minutes before weak convergence appeared (if it did at all), it is recommended that, with the environmental sounding in mind, forecasters should carefully watch for the peak in the storm's development. Even if the peak has not occurred, an increase in the reflectivity to a value indicating severe surface winds is important warning guidance. It is suggested that warning forecasters in mountainous areas (or other regions where dry microburst potential is high) keep a copy of Srivastava's GPT close by their warning system workstation for quick reference.

Several factors that may affect the accuracy of the gust prediction technique are (a) departure of the local terrain height from the assumed downdraft base of 850 mb, (b) near-surface superadiabatic lapse rates, and/or (c) increased surface moisture causing an increase in virtual temperature. Increased vertical depth would allow a downdraft to accelerate longer and thereby generate a higher downdraft velocity/peak gust than predicted by Srivastava's GPT. The opposite would be true if the local terrain is above 850 mb. However, even in the absence of item (a), items (b) and (c) alone or together would produce a stronger wind gust than predicted due to the decreased density of the boundary layer air which would result in greater negative buoyancy of the downdraft and downward acceleration. For reflectivity values >50 dBZ above the freezing level, hail/graupel contamination must be considered which will result in fictitiously high dBZ values and a correspondingly overestimate of peak wind gusts. Finally, the WSR-88D radar system should be operated in Volume Coverage Pattern 11 (VCP 11 = 14 elevation scans in 5 minutes) to maximize its storm detection capability in both time and space due to the very short-lived nature (i.e., "pulse" type) of dry microburst thunderstorms.

The use of new cell trends in the Build 9 SCIT algorithm will be helpful only if the cell is identified as a cell. Since the default SCIT thresholds are set fairly high, trends may not be available for low-reflectivity storms. A reduction of the SCIT thresholds will greatly increase the number of cells detected. It is not recommended to reduce SCIT thresholds operationally until the cells can be ranked in the cell table through the addition of the GPT to the algorithms.

Summary

Data during two dry microburst events on different days were compared to results from Srivastava's gust prediction technique. The technique uses a SCLR and peak reflectivities above cloud base to predict a surface gust. Predicted peak surface wind gusts were very close to measured wind gusts. Based on observed core descent rates of ~1000 ft per minute, the core aloft prediction should yield lead times of 15 minutes or more.

Default storm cell identification and detection algorithm thresholds failed to detect the cells for the purpose of monitoring trends in reflectivity. The minimum threshold of 30 dBZ was reduced to 16 dBZ. This allowed detection of the cells thus providing forecasters with cell

trends. However, the resultant increase in the total number of cells identified means that ranking in the cell table based on potential for severe weather is important.

References

Brown, J. M., K. R. Knupp and F. Caracena, 1982: Destructive winds from shallow, high-based cumulonimbi. Preprints, 12th Conf. On Severe Local Storms, San Antonio. Amer. Meteor. Soc., 272-275.

Proctor, F. H. and R. L. Bowles, 1992: Three-dimensional simulation of the Denver 11 July 1988 microburst-producing storm. *Meteor. and Atmos. Phys.,* **49,** 107-124.

Roberts, R. D., and J. W. Wilson, 1989: A proposed microburst nowcasting procedure using single-Doppler radar. *J. Appl. Meteor.,* **28,** 285-303.

Stewart, S. R., 1991a: The prediction of pulse-type thunderstorm gusts using vertically integrated liquid water content (VIL) and the cloud top penetrative downdraft mechanism. *NCAA Tech. Memo. NWS SR-136*, 20 pp.

_____, 1991b: The Oklahoma City, OK (Will Rogers World Airport) severe wet microburst event of 27 Sep 1986 – Use of a potential gust forecast technique. *Postprints*, National Weather Service Aviation Workshop, Kansas City, MO, Dec. 10-13, *NCAA Tech. Memo. NWS CR-102*, 199-207.

_____, 1996: Wet microbursts - Predicting peak wind gusts associated with summertime pulse-type thunderstorms. *Preprints,* 15th Conf. On WA&F, 324-327.

Srivastava, R. C., 1985: A simple model of evaporatively-driven downdraft: Application to microburst downdraft. *J. Atmos. Sci.,* **42,** 1004-1022.

Vasiloff, S. V., 1997: Microburst prediction and detection. NWS WR Technical Attachment TA97-21. WR Homepage.

Vasiloff, S. V., and D. Hogan, 1997: Another example of a dry microburst. NWS WR Technical Attachment TA97-28. WR Homepage.

Acknowledgments

Thanks to Michael Wee, Mark Benner, and Kevin Thomas (all of NSSL) for installation and maintenance of the WDSS at SLC. NSSL's WATADS was used in the data analysis.

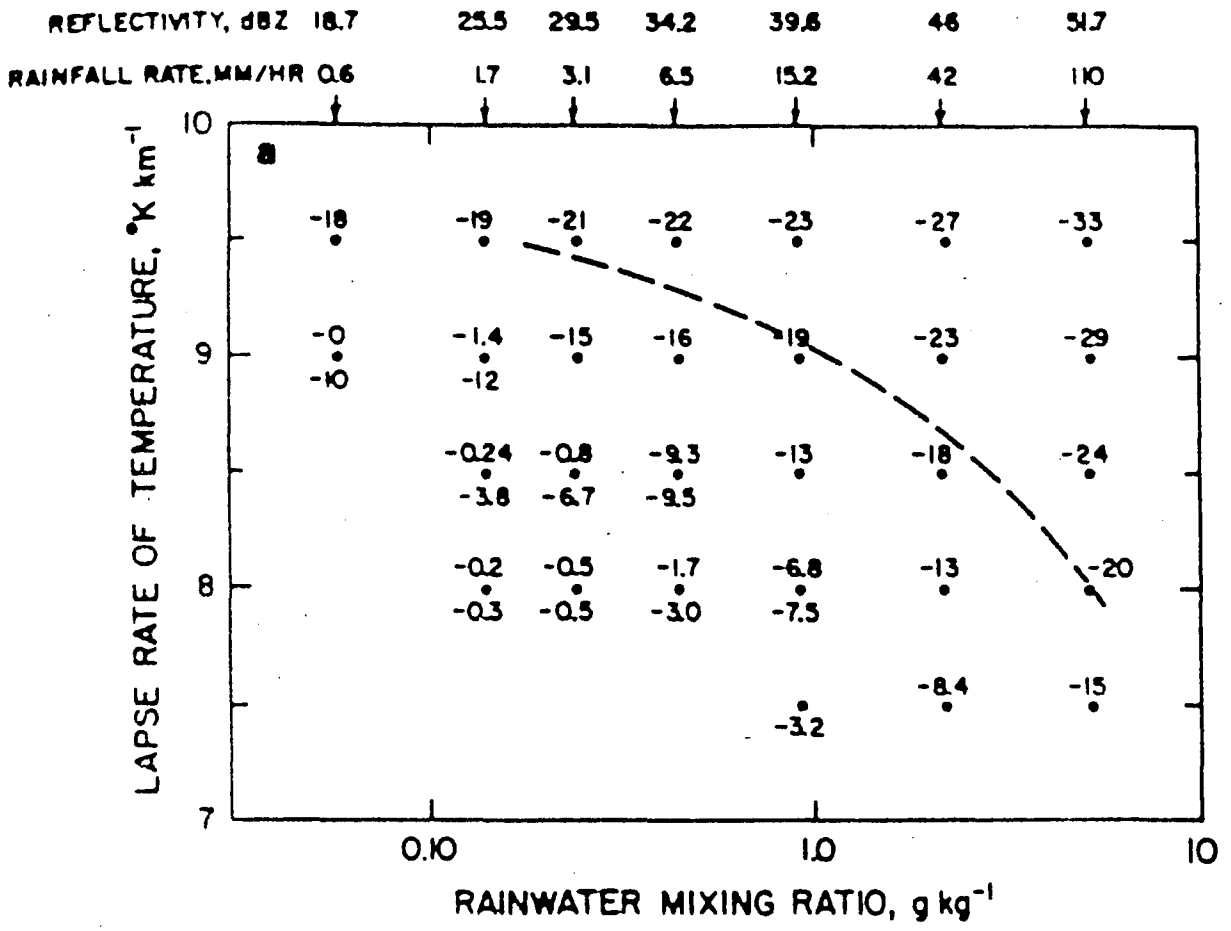

Figure 1. Predicted surface wind gusts (ms^{-1}) as a function of reflectivity and sub-cloud lapse rate (from Srivastava 1985). The dashed line separates severe from non-severe gust predictions.

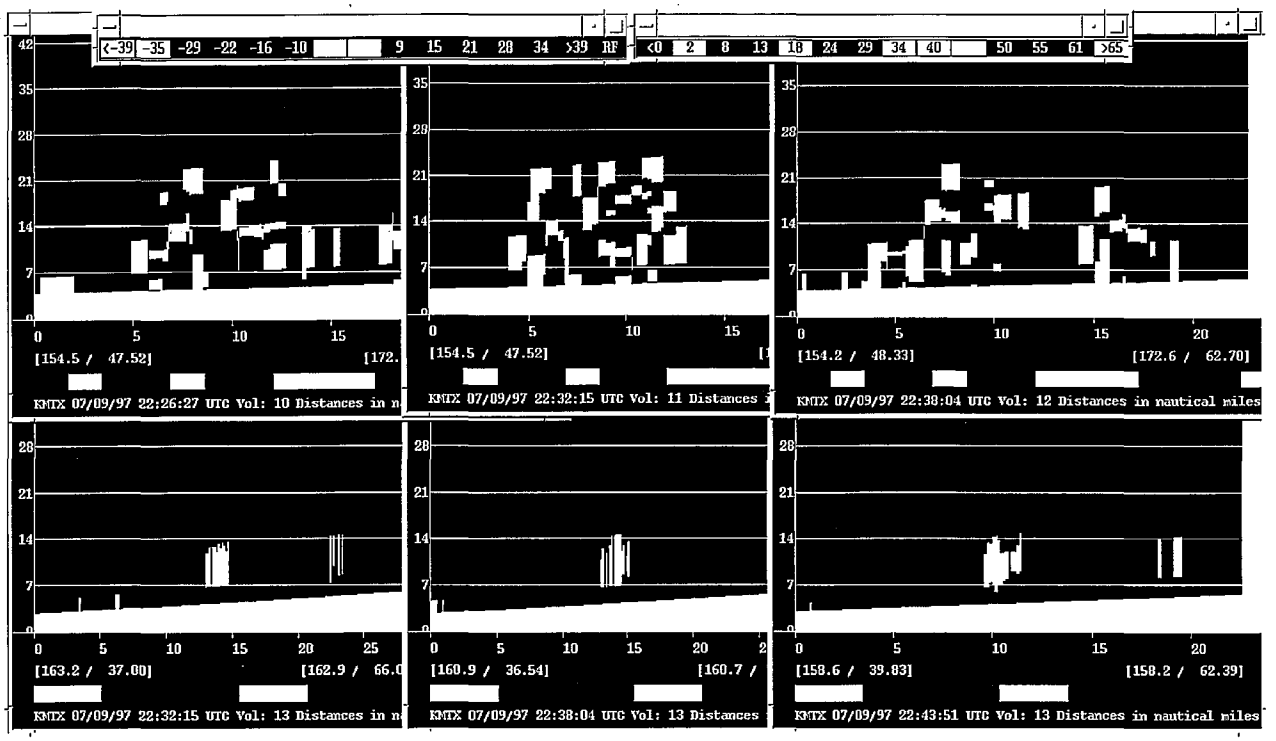

Figure 2. Sequence of vertical cross sections for the 9 July 1997 cell. Reflectivity is on the top and radial velocity in on the bottom. The reflectivity sections are oriented along the path of the cell motion. Radial velocity sections are radially-oriented through the cell.

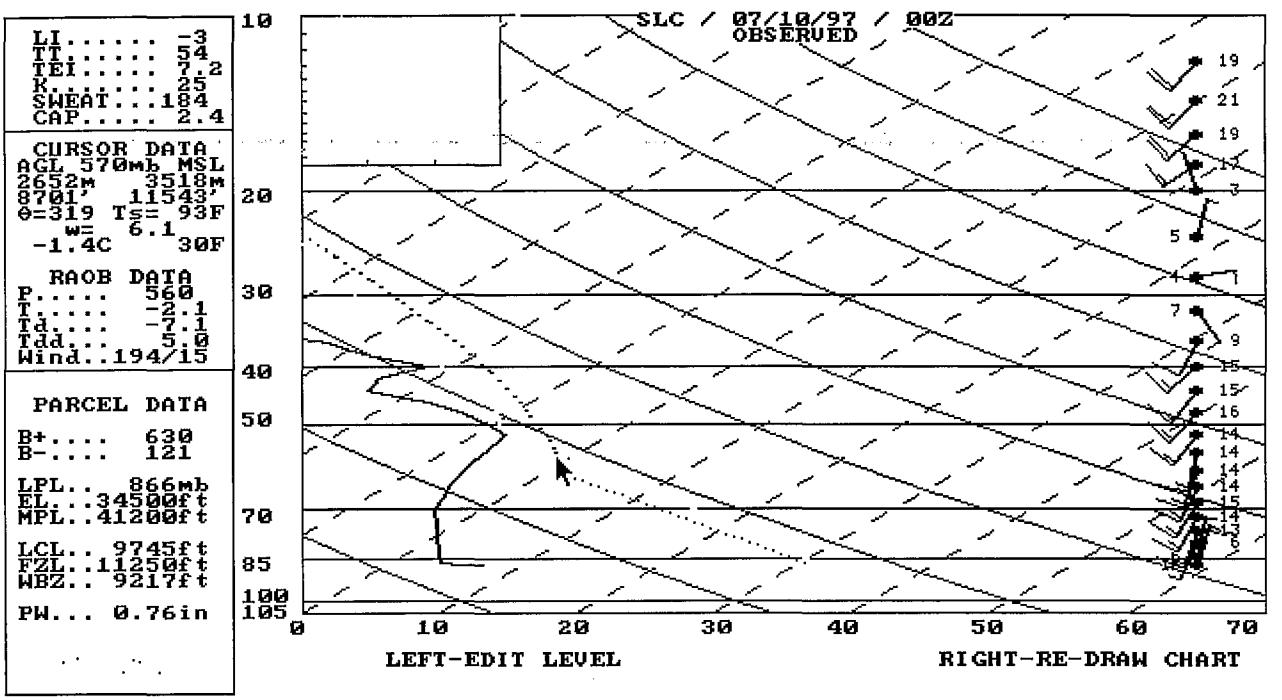

Figure 3. 0000 UTC 10 July 1997 sounding from SLC.

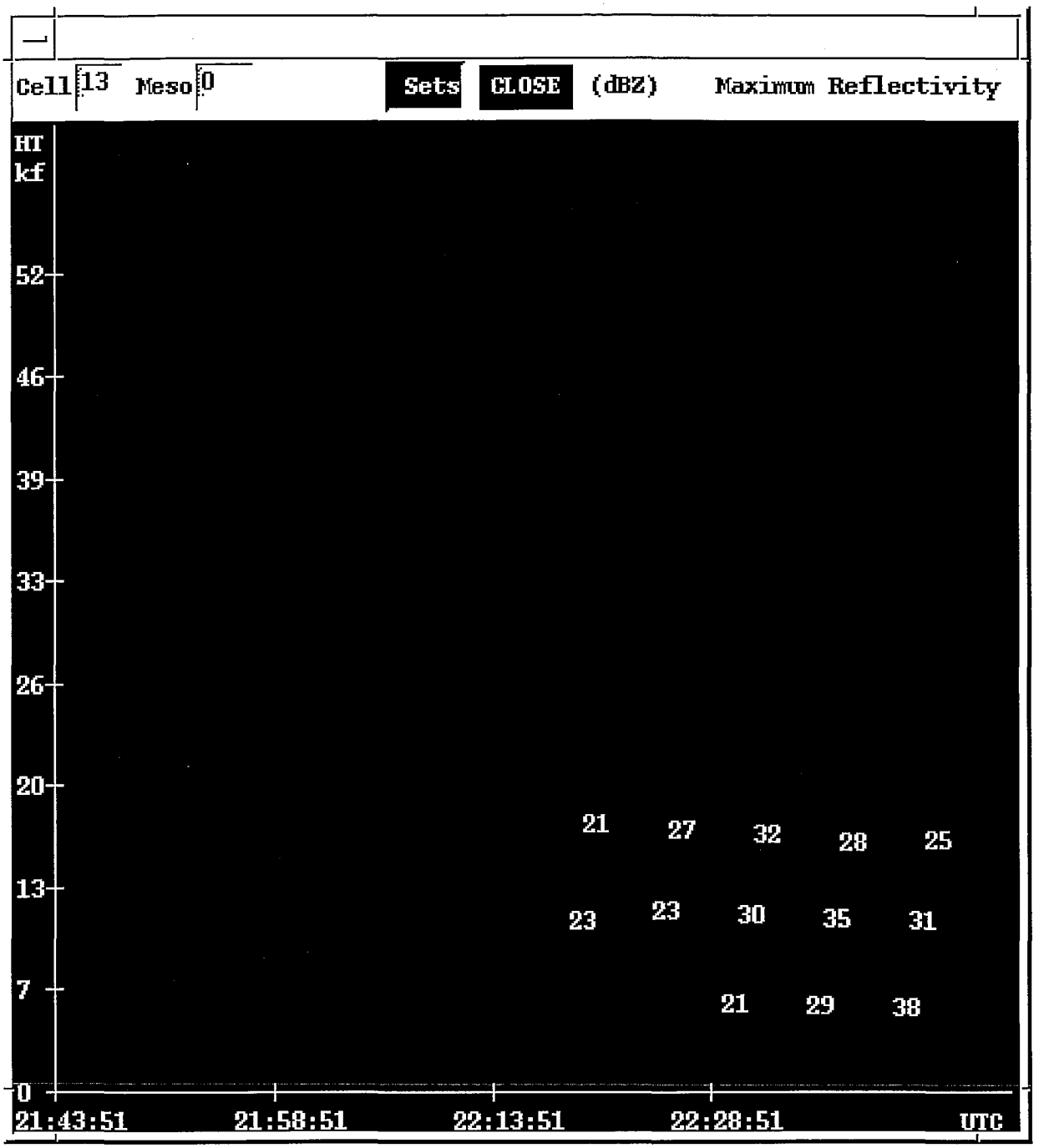

Figure 4. Time-height trend of reflectivity for the 9 July 1997 cell. Heights are above the radar.

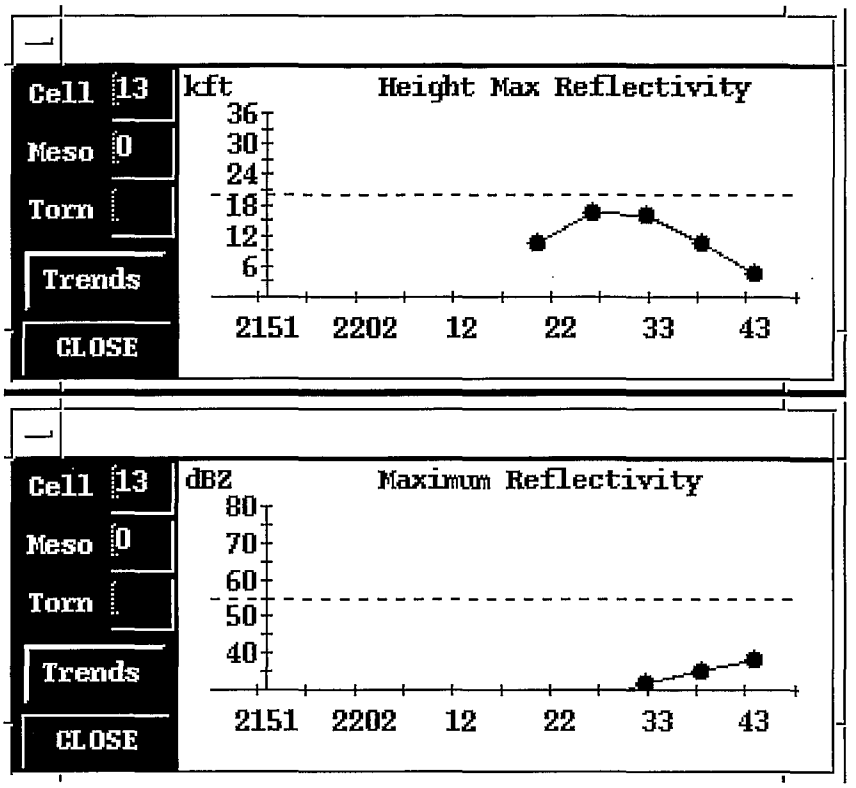

Figure 5. Trends of the height of maximum reflectivity (top) and maximum reflectivity (bottom) for the 9 July cell.

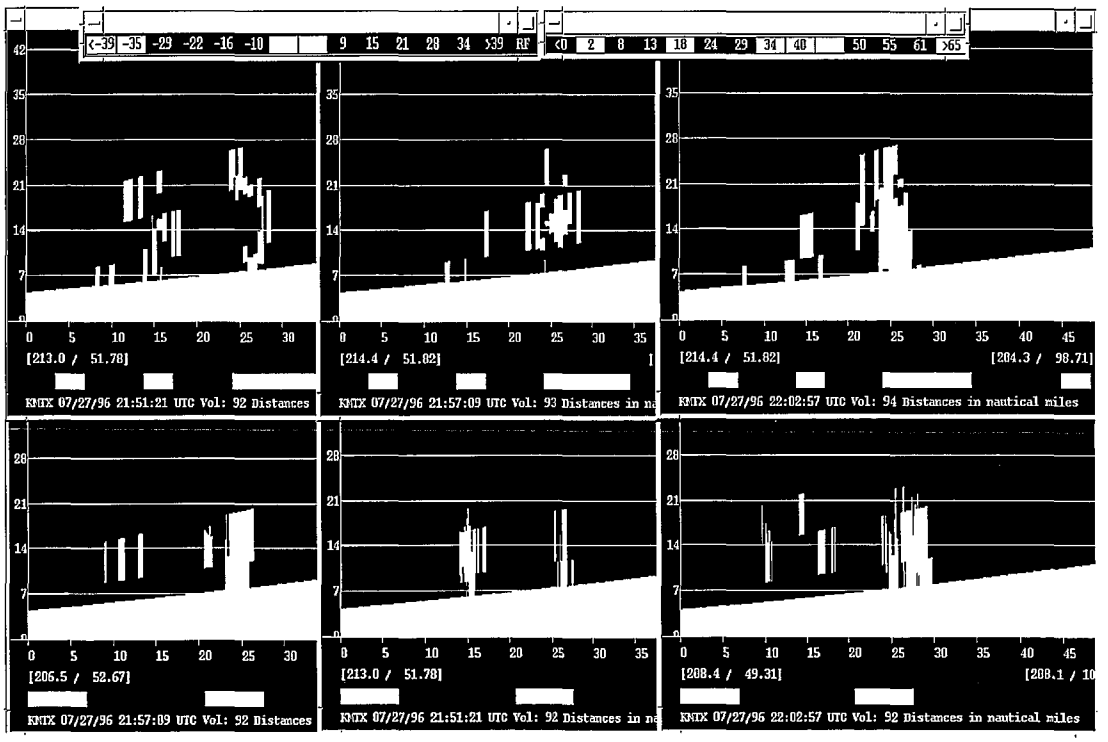

Figure 6. As in Fig. 2 except for the 27 July 1996 cell.

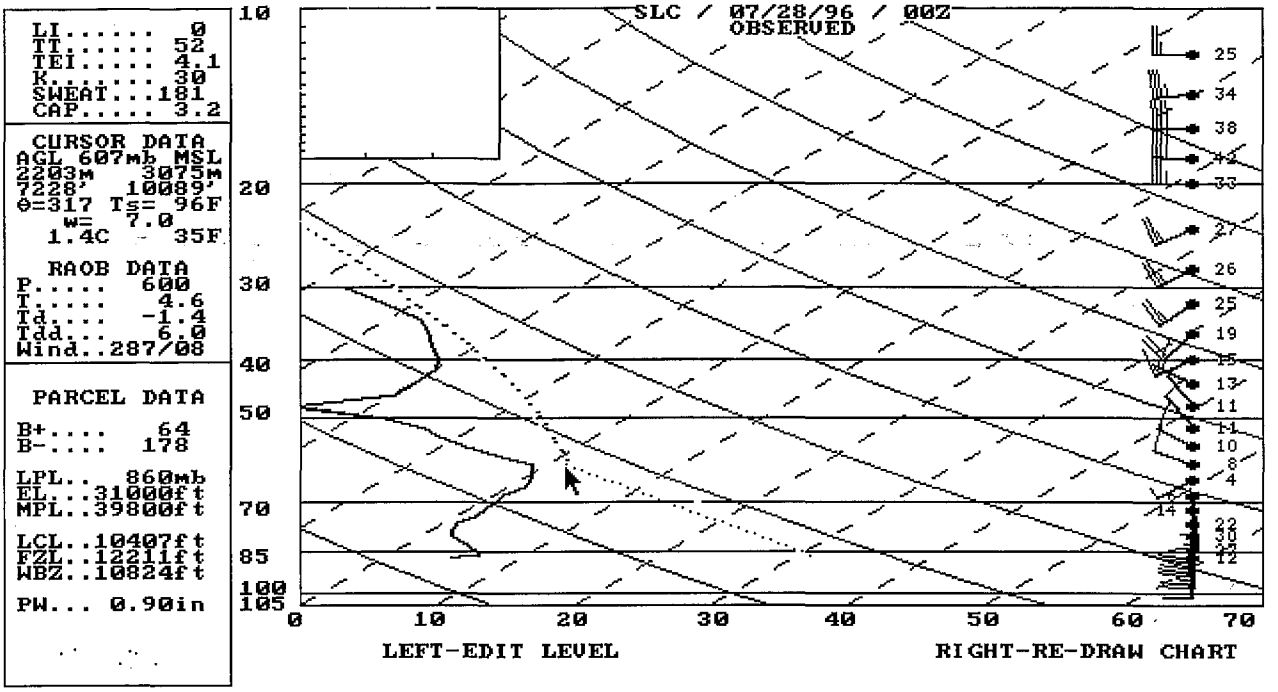

Figure 7. As in Fig. 3 except for 28 July 1996.

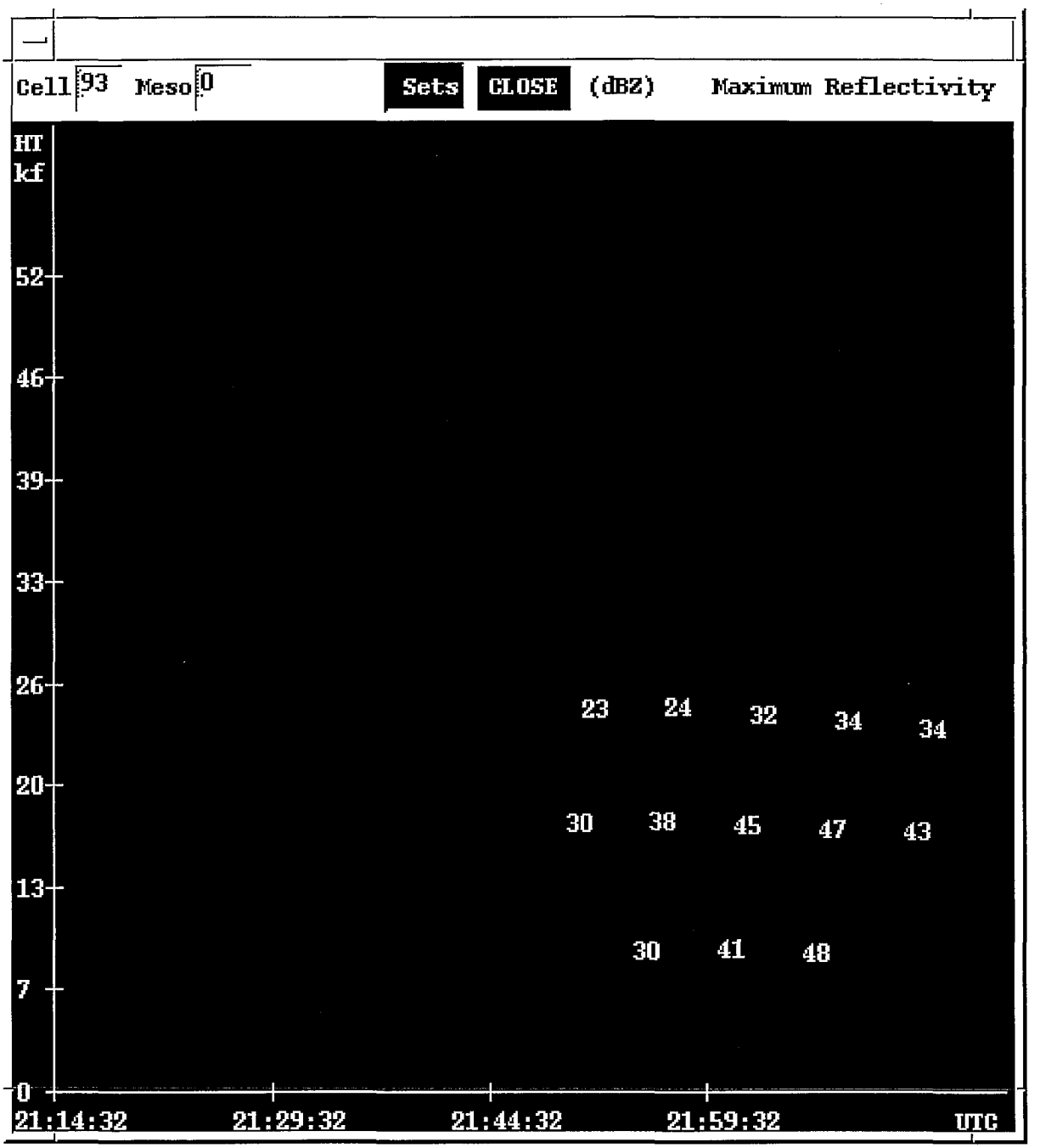

Figure 8. As in Fig. 4 except for the 27 July 1996 cell.

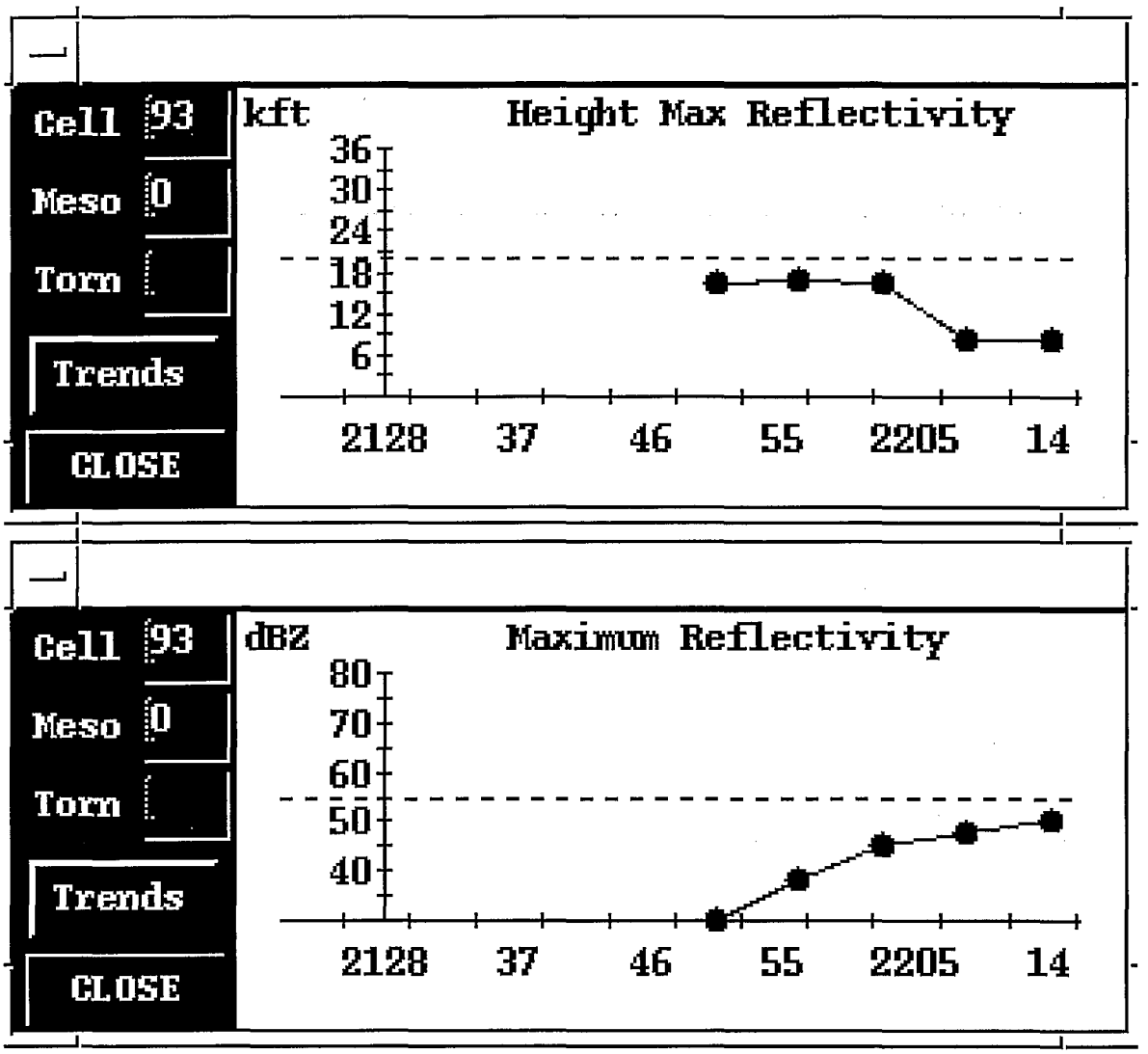

Figure 9. As in Fig. 5 except for the 27 July 1996 cell.

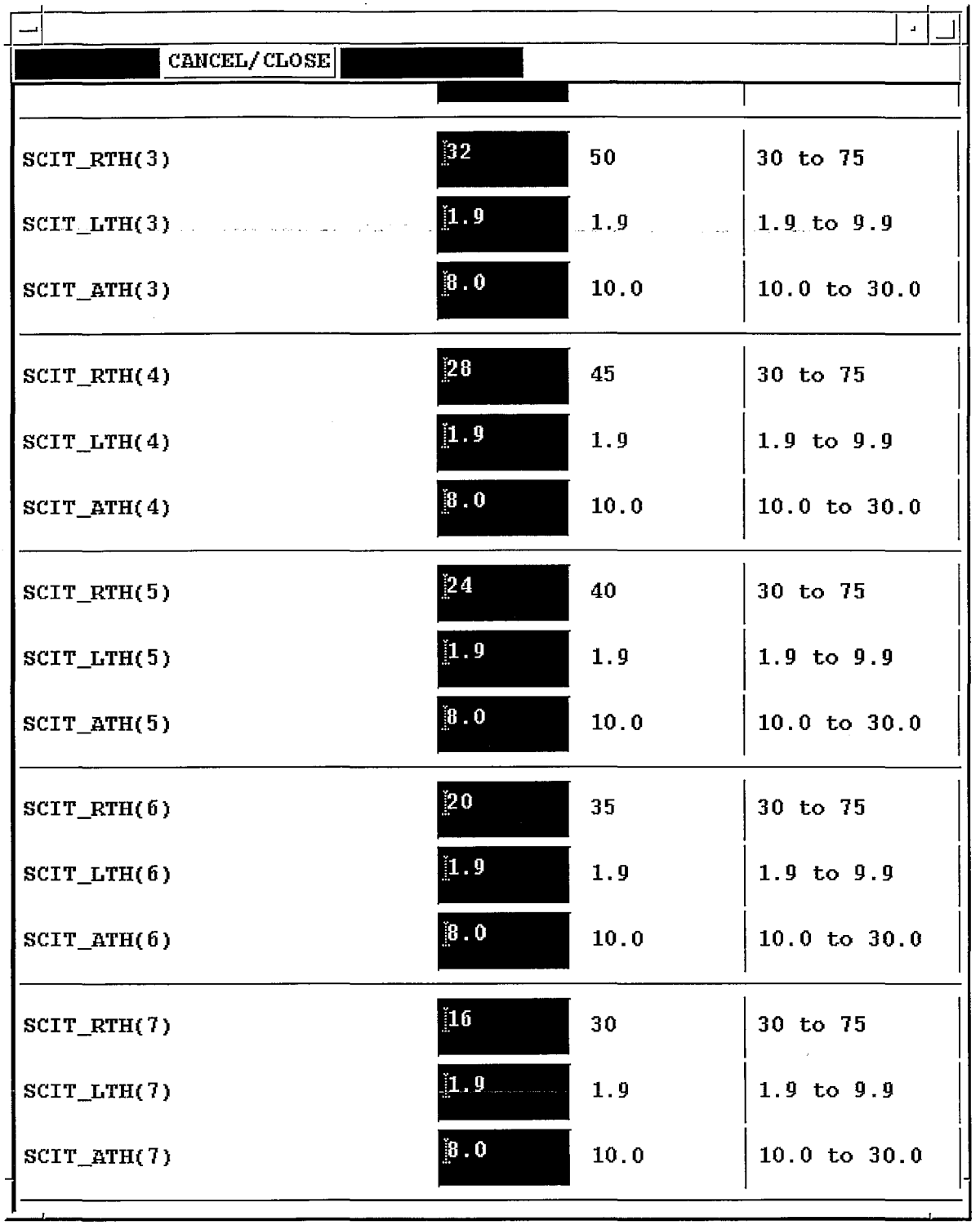

Figure 10. Window from WATADS9.0 showing the lower 5 of 7 reflectivity thresholds (SCIT_RTH) used in to define a cell in the SCIT algorithm. Numbers in the first column were used in the SCIT threshold test. The next column contains default values. The last column shows the allowable range of values. Note that the numbers used in the test are below the minimum allowable values. This is accomplished by manually editing the ssaparm.dat file.

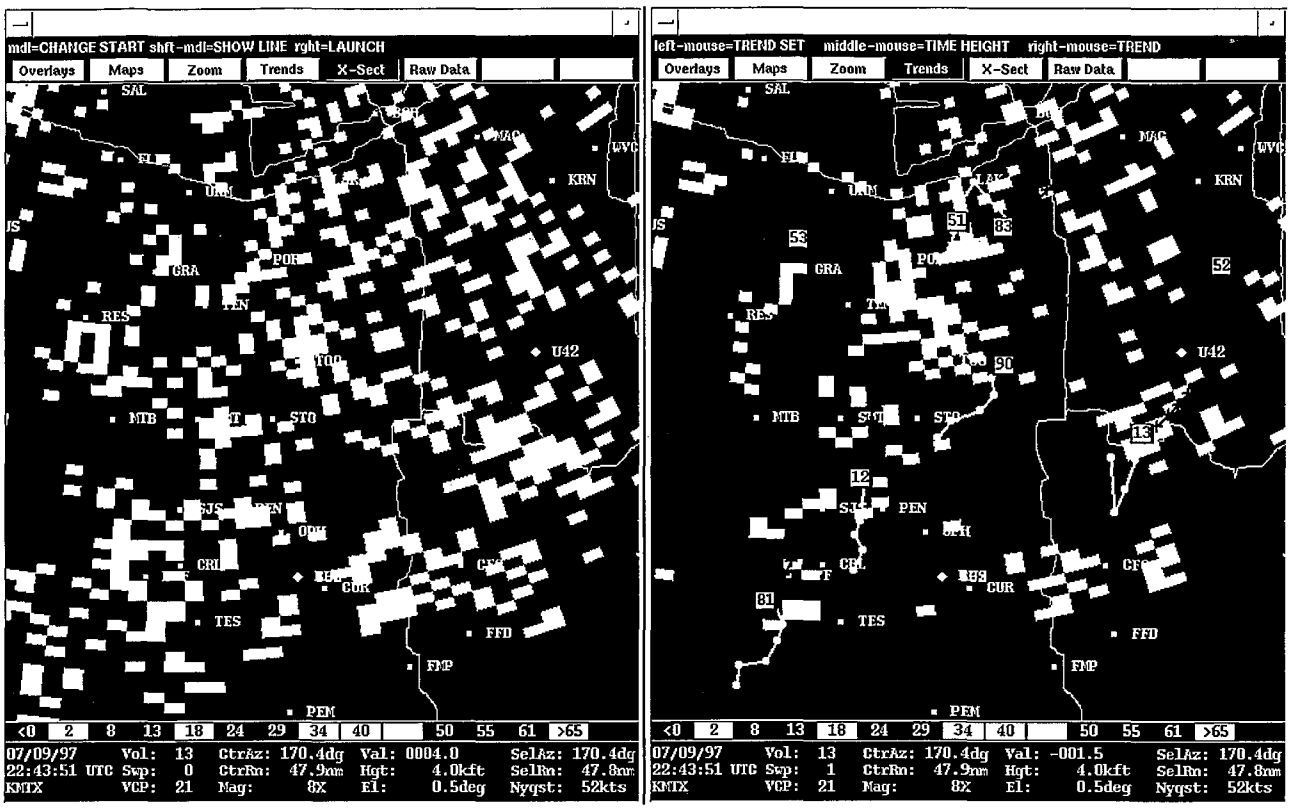

Figure 11. Composite reflectivity (left) and 0.5 deg reflectivity (right) for the 9 July case. Cell tracks and detection icons are on the right. The white dots are previous cell locations and the purple lines are the extrapolated forecast motions.

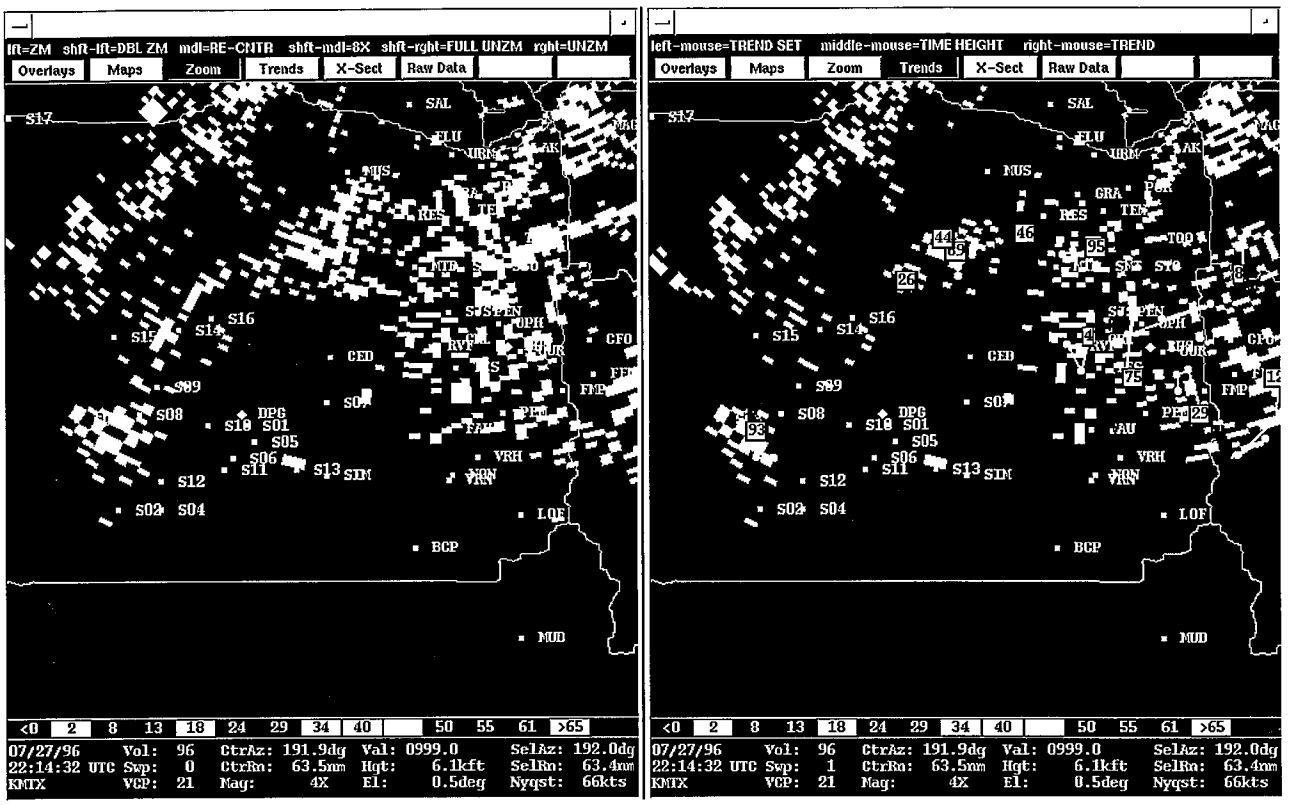

Figure 12. As in Fig. 11 except for 27 July 1996 case. The Dugway mesonet site IDs begin with the letter "S."